Chilean J. Agric. Anim. Sci. (2026) 42(1):113-126.
https://doi.org/10.29393/CHJAAS42-10MPDD20010

ISSN 0719-3890 online

IMPACT OF REPEATED TRAFFIC ON WHEAT STUBBLE: ASSESSING SOIL COMPACTION THROUGH PHYSICAL PROPERTIES AND PRESSURE SENSORS

Adrián G. Vallejos[1a*], Juan A. Galantini[1b2], and Pedro M. Bondía[1c]

[1a] Departamento de Agronomía. Universidad Nacional del Sur. San Andrés 800, CP 8000 Bahía Blanca, Argentina
https://orcid.org/0000-0003-3761-7568
[1b] Departamento de Agronomía, Universidad Nacional del Sur, San Andrés 800, (8000) Bahía Blanca, Argentina
https://orcid.org/0000-0002-4536-8605
[1c] Departamento de Agronomía. Universidad Nacional del Sur. San Andrés 800, CP 8000 Bahía Blanca, Argentina
https://orcid.org/0000-0002-1790-2620
[2] Comisión de Investigaciones Científicas (CIC). CERZOS. Bahía Blanca Argentina.
* Corresponding author: avallejo@criba.edu.ar

ABSTRACT

Soil compaction is a major driver of soil degradation, expressed as a reduction in soil volume and an increase in bulk density (BD), primarily due to porosity loss. Given the agronomic and ecological importance of pore-size distribution, this study assessed the effects of different traffic intensities associated with grain hauling in a no-tillage wheat stubble field. Three treatments were established: no traffic (NT), one pass (1P) of a tractor-grain cart combination, and two passes (2P) of the same equipment combination. The evaluated parameters included soil moisture at the time of traffic (SM), bulk density (BD), degree of compactness (DG), soil water retention curve (SWRC), pore-size distribution, S-index (S), and stress propagation measured using pressure sensors. Under 1P, BD significantly increased down to 15 cm depth, whereas under 2P the effect extended to 20–35 cm depth. Total porosity declined to 25 cm under 1P and to 30 cm depth under 2P. The S-index dropped below critical threshold values between 10 and 25 cm under 2P, consistent with observed reductions in porosity. DG values aligned with S vs. DG curve inflections. Pressure sensors failed to decompress at 30 cm under 2P, indicating persistent compaction. These findings confirm the reliability of the S as a soil quality indicator and highlight the potential of pressure sensors for detecting soil deformation under traffic-induced stresses.

Keywords: Multipass, S-index, porosity change, soil water retention curve.

INTRODUCTION

Compaction is a key driver of soil degradation, manifesting as a reduction in volume and an increase in bulk density (BD) due to porosity loss. These alterations change pore shape, distribution, and size, directly impacting aeration and infiltration capacity. Consequently, soil compaction induces substantial changes in physical, chemical, and biological processes that influence crop production and create conditions conducive to increased surface runoff and erosion (Fu et al., 2019).

The vehicular traffic is the main cause of soil

Received: January 26, 2026 Accepted: April 13, 2026

compaction. Surface compaction is governed by tire contact (i.e., load on the tire divided by the contact area), while subsurface compaction is mainly drive by axle load (Schjønning et al., 2016; Wang et al., 2022)

The frequency of traffic, axle load, and tire-soil contact pressure determine the degree of soil compactness (DC) and, consequently, crop production (Botta et al., 2018; Nawaz et al., 2023). Additionally, soil compaction can be cumulative in nature (Seehusen et al., 2019; Augustin et al., 2020). In particular, Seehusen et al. (2019) highlight the fact that using multiple wheels with comparatively low wheel loads can be more damaging than using a single wheel with a higher load, especially in the topsoil layer.

The trend towards reducing crop establishment and protection costs has led agricultural machinery manufacturers to increase the working capacity of equipment (Antille et al., 2019).

This increased capacity inevitably comes with greater weight, which can lead to long-term subsoil compaction issues (Keller et al., 2019).

Argentina has not been exempt from this trend. Currently, there is a shift toward larger harvesters equipped with engines exceeding 550 HP, dual tires, and grain tanks with capacities greater than 10,000 L. These machines can exceed a total weight of 30 Mg (Antille et al., 2019), promoting soil compaction.

Currently, single-axle grain carts with a capacity of 14-18 Mg and double-axle carts with 20-50 Mg are commonly used, while tractor weights marketed in recent years range from 7.5 to 10 Mg. These axle loads exceed the 3 Mg per wheel threshold proposed by Schjønning et al. (2016), thereby increasing the risk of compaction extending into deeper subsoil layers, where it may be highly persistent or even permanent.

Traffic intensity (number of passes) has remained stable or increased with the use of heavier equipment, thus increasing the risk of soil compaction (Augustin et al., 2020).

As axle load is the cause of subsurface compaction, this issue is particularly critical because mechanical loosening is often costly and of limited effectiveness; in some cases, it may even have negative effects on soil structure (Schjønning et al., 2016)

No-till generally leads to an increase in BD due to the cumulative effect of machinery traffic and natural particle rearrangement (Seehusen et al., 2019, Augustin et al., 2020).

As previously mentioned, compaction by traffic reduces soil volume and thus pore space and water retention in soil. However, the redistribution of pore size can prevent volume change (ten Damme et al. 2021; Yadav et al., 2020). When the soil is moist, pores can become deformed and reduced in diameter; under drier conditions, aggregates fracture, generating particles that fill the spaces and create smaller pores (Startsev and McNabb, 2001). In this way, macropores collapse, increasing the volume of micropores (Aschonitis et al., 2015; Fu et al., 2019, Valente et al., 2025), creating a dynamic process where the destruction of larger diameter pores creates smaller diameter pores (Yadav et al., 2020). This has a significant effect on water transmission and storage in the soil (Guenette et al., 2019). However, some authors do not report increases in microporosity following the passage of machinery (Bellora et al., 2023; Fouladidorhani et al., 2025).

To compare the compaction of different soils, a relative or normalized density value should be used (Naderi-Boldaji and Keller, 2016). This value can be obtained by referencing a maximum BD value. Carter (1990) proposed the maximum density from the Proctor test as a suitable reference. A strong positive correlation between the degree of compactness (DC) and ln(1/S) has been suggested (Naderi-Boldaji and Keller, 2016; Al-Kayssi, 2021).

Dexter (2004) proposed the use of the S value as an index of soil physical quality for comparing soils under different management conditions. This index is derived from the soil water retention curve (SWRC), represented as the gravimetric water content against the natural logarithm of the absolute matric potential of the soil, corresponding to the inflection point.

The S-index derived from the SWRC has demonstrated sensitivity in detecting alterations in soil structure (Lima et al., 2019; da Luz et al., 2020; Fernández et al., 2021). Under different compaction conditions, it has also shown a high correlation with soil physical parameters (Aschonitis et al., 2015).

The S-index divides soil porosity into fine (textural) and coarse (structural) pores. According to Dexter (2004), the S value indicates the extent to which soil porosity is concentrated within a limited range of pores; therefore, physical soil degradation will result in a decrease in the S value. Therefore, Dexter (2004) suggested a threshold value of approximately $S > 0.035$ for soils with good structural quality, with lower values indicating poorer structural conditions. Furthermore, soils with $S < 0.02$ were classified as having very poor physical quality.

One approach to study traffic-induced forces in soils is the use of electronic transducers and pressure sensors. This method enables the assessment of the relative effects of key factors, including load, soil texture, and moisture

content, and surface cover. Pressure sensors offer the additional advantage of recording residual compaction caused by traffic. At this stage, soil deformation becomes irreversible, and the probe remains pressurized after the passage of the tire (Raper and Arriaga, 2007).

In the southern Pampean region of Argentina, production systems are based on mixed crop-livestock farming, with a focus on wheat, winter forage cereals, soybean, and sunflower. During the harvest of the these crops, soils are often wet and have low surface cover, making them susceptible to compaction by harvesting machinery. As noted previously, mechanical decompaction is costly and not always effective; therefore, preventing soil compaction is a crucial factor.

Information on soil behavior under no-till systems subjected to machinery traffic remains limited. Although traffic intensity is generally lower in no-till systems, the use of large and heavy machinery can lead to surface or subsurface compaction, particularly under conditions of high soil moisture. Therefore, evaluating the effects of mechanical traffic on soil physical properties is essential to ensure the long-term sustainability of no-till systems (Botta et al., 2022).

Given the productive and ecological significance of changes in pore size distribution and BD, the objectives of this study were to: (i) evaluate the effects of different intensities of tractor- grain cart traffic on soil deformation and changes in soil physical properties, including bulk density (BD), pore size distribution, and soil water retention characteristics); (ii) assess the sensitivity of pressure sensors for detecting soil deformation compared to conventional indicators; and (iii) validate the upper threshold values of the degree of compactness (DC) and S-index based on the load at which residual stress is detected by pressure probes. It was hypothesized that increasing traffic intensity induces soil compaction, manifested as increased BD, alterations in pore-size distribution, and reduced S-index values. Furthermore, pressure sensors are expected to be more sensitive than BD measurements for detecting soil deformation, and the critical thresholds of DC and S-index reported in the literature are anticipated to correspond to the onset of soil deformation detected by these sensors.

MATERIALS AND METHODS

The trial was conducted on a farm near the town of Espartillar (37° 11′ 19″ S, 62° 26′ 59″ W) in the Saavedra district, Buenos Aires Province, Argentina. The soil was classified as a petrocalcic Paleustoll with a loamy texture (Table 1). The field was under fallow in preparation for wheat sowing, following two consecutive years of wheat under no-till cultivation.

For the traffic experiment, a 140 HP tractor (Deutz AX 5.140®) with single-wheel drive and a static weight of 5,980 kg, was used. The tractor was equipped with front tires (1,100-16; inflation pressure 220 kPa) and rear tires (23.1-30; inflation pressure 110 kPa). Grain cart fitted with front tires (16.9-24; inflation pressure 207 kPa) and rear tires (23.1-30; inflation pressure 220 kPa) was loaded with maize grains, resulting in a gross weight of 16,090 kg. Traffic intensity was 105.3 Mg km ha^{-1} for 1 pass (1P) and 210.6 Mg km ha^{-1} for 2 passes (2P), calculated following Håkansson (2005).

Experimental design

The trial evaluated three traffic intensities using a tractor–grain cart combination: no traffic (NT), 1P, and 2P. A completely randomized block design was used, with three blocks and three treatments, resulting in a total of nine experimental units. Each experimental unit consisted of a 20 m tractor track.

Soil samples for the determination of the evaluated edaphic properties were collected from four depth intervals: 2–7 cm (Ap horizon), 10–15 cm (A_2, plow pan), 20–25 cm (A_2 horizon), and 30–35 cm (AC horizon).

Data were analyzed using analysis of variance (ANOVA), and mean comparisons were performed using Fisher's LSD test at a 5% significance level. As θ_i values did not follow a normal distribution, the nonparametric Kruskal–Wallis test was applied. Statistical analyses were

Table 1. Soil characteristics.

Horizon	Depth (cm)	Clay	Silt (%)	Sand	Texture
Ap	0 to 10	23.2	37.6	39.1	Loam
A2	10 to 24	23.7	37.6	38.8	Loam
A3	24 to 39	36.5	36.5	41.6	Clay
AC	39 to 67	-	-	-	
C	67 to 115	-	-	-	
Petrocalcic	+ 115				

conducted using INFOSTAT software (Di Rienzo et al., 2019).

Field and laboratory assessments

At the beginning of the trial, the wheel path was marked, and then five undisturbed samples were taken (using steel cylinders of known volume) for each depth evaluated in each of the experimental units, thus completing the sampling of the NT. Subsequently, the equipment passed along the same track and sampling was repeated at the center of the track for 1P. The equipment was then passed over the plots a second time, and sampling was conducted for the 2P treatment.

The samples were extracted at specific depths: 2-7 cm, 10-15 cm, 20-25 cm, and 30-35 cm. Following collection, they were carefully covered to safeguard their integrity until processing. Upon arrival at the laboratory, the samples were weighed to determine their initial wet weight. Subsequently, they were carefully prepared and systematically saturated over a 24-hour period using a glass humidifier, with water added incrementally to ensure controlled and gradual moisture uptake.

The SWRC for each sample was determined at matric potentials of 0.98, 9.8, 33, 100, and 300 kPa using pressure cells and a membrane apparatus. After equilibrium was reached, samples were weighed and then oven-dried at 105 °C. The wilting point (WP) was obtained at 1500KPa using soil passed through a 2 mm sieve. BD was determined using standard procedures. Gravimetric water content was calculated at each tension (Klute, 1986), and soil moisture (SM) at the time of sampling was also recorded.

Maximum bulk density (BDMax) was determined using the Proctor test for the topsoil (0-20 cm) and the subsoil (20-40 cm) layers.

Critical soil moisture (CSM) was defined as the moisture content at which BDMax is achieved, as determined from the Proctor test.

The degree of compactness (DC) was calculated for the topsoil (0-20 cm) and the subsurface layer (25-40 cm) as the ratio between the BD of each sample and the corresponding BDMax obtained from the Proctor test (Carter, 1990).

Pore-size distribution was defined according to Iglesias et al. (2014), based on functional differences related to water movement and storage capacity. The following pore sizes were evaluated: (i) Macropores, mesopores, and micropores.

Macropores were defined as pores larger than 9 μm, which facilitate primary water flow, infiltration, and drainage, thus exerting greater control over soil aeration. They were further subdivided into large macropores (greater than 30 μm; BMP), and small macropores (30-9 μm; SMP), reflecting differences in drainage characteristics.

Mesopores were defined as pores with diameters between 9 and 0.2 μm, corresponding to the field capacity (FC) and permanent wilting point (WP) limits, which are particularly relevant for water storage and microbial activity.

Micropores were defined as pores with diameters smaller than 0.2 μm, which retain water that is largely unavailable to plants.

The effective pore diameter (D) was estimated in each undisturbed soil sample from the SWRC as:

$$D = 2r = 30.0 \times 10^{-6} \times h^{-1}$$

where h is the pressure height in meters and r is the radius.

FC and WP were obtained from the SWRC at pressures of 33 kPa and 1500 kPa, respectively, with WP obtained using disturbed samples.

The S-index was calculated from the SWRC obtained at the evaluated matric potentials using pressure cells and a membrane apparatus (Klute, 1986). The water retention data were fitted using the equation proposed by van Genuchten (1980), as follows:

$$\theta = (\theta sat - \theta res) \times [1 + (\alpha h)n] - m + \theta res$$

where:
θ = volumetric moisture content,
θsat = volumetric moisture content at saturation,
θres = volumetric moisture content at permanent wilting point,
h = soil matric potential,
α, n, and m are model adjustment parameters.

For the calculation of S, the equation proposed by Dexter (2004) was used:

$$S = -n\,(\theta sat - \theta res) \times [1 + (1/\mathrm{m})] - (1 + \mathrm{m})$$

The moisture at the inflection point of the SWRC was calculated using the following equation (Dexter, 2004):

$$\theta i = (\theta sat - \theta res) \times [1 + (1/\mathrm{m})] - \mathrm{m} + \theta\mathrm{res}$$

Vertical load measurements were conducted using a device developed by Pozzolo et al. (2008), consisting of eight electronic pressure transducers, each equipped with a deformable pressure probe inserted into the soil profile. The probes were connected via pressure hoses (3.2 mm inner diameter) to an electronic pressure transducer module. The pressure probes used in this study were specifically developed for this purpose (Fig. 1).

Fig. 1. Installation of pressure probes in the soil profile through a test pit (a), and detailed view of the pressure probe acting as an interface between the soil and the electronic pressure transducer (b).

Four of the eight electronic pressure transducers were less sensitive, with a measurement range of 0-100 kPa, and were classified as high-pressure sensors (HPS). The remaining sensors, with higher sensitivity and a measurement range of 0-10 kPa were classified as low-pressure sensors (LPS). The transducer was connected to a computer via a serial port for continuous data acquisition.

Pressure probes (28 cm in length) were inserted horizontally into the soil. This procedure involved excavating a soil pit (150 cm long and 100 cm deep), followed by horizontal drilling into the pit wall to a depth of 48 cm using a 2.8 cm drill bit and a manual drill. Subsequently, the probes were inserted and pressurized to approximately 30 kPa for HPS and 4 kPa for LPS, ensuring proper contact between the deformable unit and the surrounding soil.

Residual pressure was calculated as the mean of 10 readings recorded after the passage of the equipment.

RESULTS AND DISCUSSION

At the time of conducting the experiment, the surface layer of the soil exhibited moisture levels close to FC, whereas the deeper soil layers were comparatively dry, approaching the WP (Table 2).

In the surface layer, BD values in the traffic treatments did not significantly differ from each other but were statistically distinct from those of the control (Fig. 2). In the 2-7 cm layer, BD increased by 13% in the traffic treatments compared to the control, while in the 10-15 cm layer (plow pan), the increase was 4.5%. Nawaz et al. (2023) reported soil densification in the plow pan caused by repeated traffic with low axle loads. Similarly, Botta et al. (2018) observed low-magnitude densification in the plow pan, attributing this effect to pre-existing compaction in that layer. Notably, the SM values in the present study exceeded FC, suggesting that under drier conditions, closer to CSM, BD values could potentially increase further.

At depths of 20-25 cm and 30-35 cm, similar behavior was observed for the 1P treatment, with no significant differences in BD compared to the control. However, the second pass of the tractor-grain cart combination led to a significant increase in BD, approximately 5% in the 20- 25 cm layer and 8% in the 30-35 cm layer.

As SM values of the subsurface were close to the WP (Table 1), under these conditions, stress transmission extends more horizontally, consequently reducing maximum pressures. In addition, the presence of compacted layers can act as support layers, protecting deeper soil horizons (Terminiello et al., 2004). This protective effect was evident after a single pass (1P) of the tractor-grain cart combination. However, after the second pass, the mitigating effects of the plow pan and the low SM were no longer apparent, suggesting that the applied loads exceeded the bearing capacity of the soil in these strata, in agreement with Keller et al. (2019).

Significant increases in BD following the second pass indicate a cumulative effect of traffic (Seehusen et al., 2019). Under the conditions of this study, the commonly recommended strategy of reducing axle load by distributing it across multiple axles (Keller and Arvidsson 2004) did not yield the expected mitigation effect. Therefore, both axle load (Schjønning et al., 2016) and traffic intensity (Seehusen et al., 2019) must be considered when evaluating the risk of subsoil compaction.

The maximum bulk density achieved from the Proctor test was 1.56 Mg m^{-3} for the 0-20 cm depth and 1.51 Mg m^{-3} for the 25-40 cm depth (Fig. 3). Based on the results, a single pass of

Table 2. Gravimetric moisture content at the beginning of the trial, at field capacity, at permanent wilting point, and at critical moisture for the studied depths.

Depth (cm)	SM (g/g)	FC (g/g)	WP (g/g)	CSM (g/g)
2 to 7	0.23	0.22	0.12	0.20
10 to 15	0.22	0.23	0.12	0.20
20 to 25	0.10	0.23	0.12	0.20
30 to 35	0.09	0.22	0.11	0.24

SM: current soil moisture; FC: field capacity at 33 kPa; WP: permanent wilting point at 1500 kPa; CSM: critical soil moisture from Proctor test.

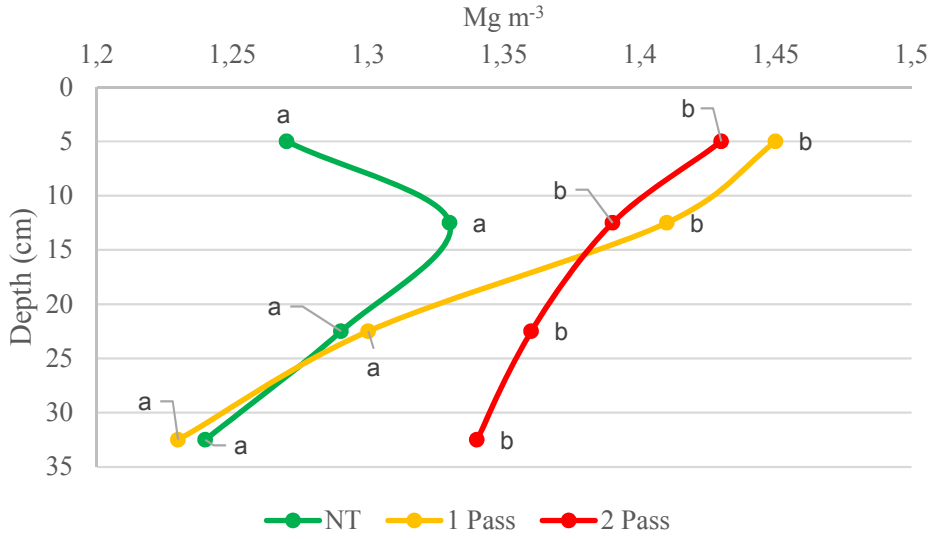

Fig. 2. Bulk density at different depths under different traffic treatments: NT (no traffic); 1 pass, and 2 passes of the tractor-grain cart combination. Means followed by the same letter are not significantly different according to Fisher's LSD test (P<0.05).

the equipment was sufficient to exceed 89% of the DC in the 1P treatment at 2-7 cm depth, and up to 35 cm in 2P treatment (Table 3). Values exceeding 89% are associated with reduced crop performance, as reported by Carter (1990) and Naderi-boldaji and Keller (2016).

In general, compaction alters pore-size distribution, leading to a decline in microporosity, while the opposite trend is observed for micro porosity (Aschonitis et al., 2015; ten Damme et al., 2021; Valente et al., 2025).

In the upper layer, a decreasing trend in volumes in BMP and SMP was observed under the traffic treatments (Fig. 4). Some of these pores were reclassified into the mesopore category, while the rest disappeared, leading to a significant reduction in saturated porosity (Table 4), consistent with the findings of Yadav et al. 2020. It should be considered that mesopores function primarily as storage pores and correspond to the range of water held under higher matric suctions. Consequently, the reduction of larger-diameter pores likely decreases both water infiltration and storage capacity (Guenette et al., 2019).

The changes in pore-size distribution among treatments explain the observed differences in BD, resulting from the reduction in pore volume mainly within water-conducting macropores (larger than 9 μm). In the 10-15 cm layer, the 2P treatment caused exhibited a significant decrease in BMP and SMP categories, with part of this pore volume redistributed into mesopores, while the remainder was lost, leading to a reduction in saturated porosity (Table 4). The effect of 1P was less pronounced than that of 2P for pores >30 μm (Fig. 4). In this case, some of these pores were redistributed to the SMP and mesopore categories. It is possible that part of the energy applied during the first pass was lost in track formation, or that drainage was insufficient to

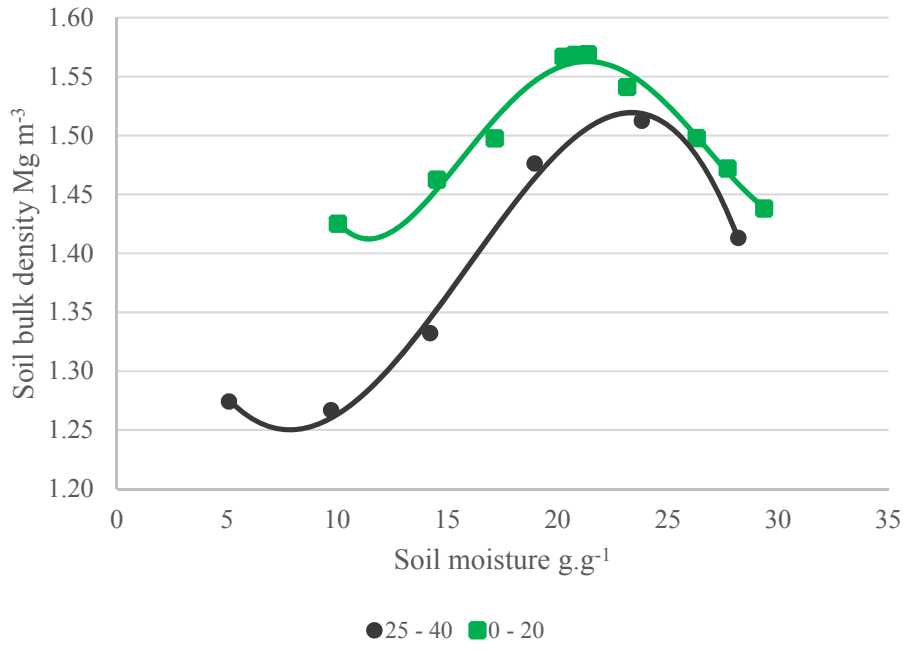

Fig. 3. Soil gravimetric moisture content at maximum compaction (BDMax) determined by Proctor tests for the 0-20 cm and 25-40 cm depths.

Table 3. Relative compaction in the 2-7 cm and 10-15 cm layers under different traffic treatments: Control (NT), one pass (1P), and two passes (2P) of the tractor-grain cart combination.

Depth cm	NT (%)	1 P (%)	2 P (%)
2 to 7	81 a	92 b	91 b
10 to 15	85 a	90 b	89 ab
20 to 25	85 a	86 ab	90 b
30 to 35	82 a	81 a	89 b

Means followed by the same letter indicate no significant differences between treatments according to Fisher's LSD test ($p < 0.05$).

fully empty the pores, thereby increasing the neutral tension of the soil due to the presence of water (Fu et al., 2019).

The BMP category exhibited the highest reduction down to 15 cm under both 1P and 2P conditions (Fig. 4a, b), in agreement with the findings of Schäffer et al. (2007) and Aschonitis et al. (2015). Although some pore categories did not show statistically significant differences down to 15 cm, plastic deformation without a net change in volume should cannot be ruled out, as it may alter continuity of the pore space (ten Damme et al., 2021). Reductions in saturated porosity were consistent with increases in BD, highlighting BD as a sensitive indicator of soil structural deformation.

In the 20-25 cm layer under 1P conditions, no traffic effect was detected, and the pore category values were consistent with BD results (Fig. 4c; Fig. 2). However, under 2P, a reduction in pore volume was observed in the drainage-related categories (BMP and SMP). No clear pore redistribution was observed, indicating that these reductions persisted and led to a significant decrease in saturated porosity compared to the control and 1P treatments, consistent with the increase in BD.

In the deepest soil layer, no effect of 1P was observed (Fig. 4d). No reductions in the studied pore-size categories were detected (Table 3), and these results were consistent with the BD values. Conversely, under 2P conditions, a significant reduction in drainage-related pore categories (BMP and SMP) was observed. No redistribution

Table 4. Distribution of pore volume (%) and saturated porosity under control (T), one pass (1P), and two passes (2P) of the tractor-grain cart combination.

	Pore categories				
	>30 µm	30 to 9 µm	9 to 0.2 µm	< 0.2 µm	Porosity
2 to 7 cm					
NT	17.74 b	6.16 b	17.85 a	10.90	50.56 b
1P	8.49 a	4.16 ab	23.04 b	10.02	45.71 a
2P	10.33 ab	2.76 a	22.39 b	10.57	46.05 a
10 to 15 cm					
NT	18.86 c	3.11 ab	17.52 a	10.97	50.46 a
1P	17.47 b	3.42 b	20.07 ab	10.28	48.51 ab
2P	11.58 a	2.02 a	22.16 b	10.46	46.22 b
20 to 25 cm					
NT	19.75 b	4.25 b	21.2 a	10.55	55.75 b
1P	19.5 b	5.84 c	17.77 ab	11.24	54.35 b
2P	12.19 a	2.21 a	21.07 b	11.2	47.38 a
30 to 35 cm					
NT	19.44 b	4.38 a	20.14 b	9.81 a	53.77 b
1P	20.14 c	5.67 b	17.84 a	10.1 b	53.75 b
2P	15.57 a	3.87 a	20.06 b	9.49 a	48.99 a

For each depth and pore size category, means followed by the same letter indicate no significant differences between treatments according to the Fisher's LSD test ($p < 0.05$).

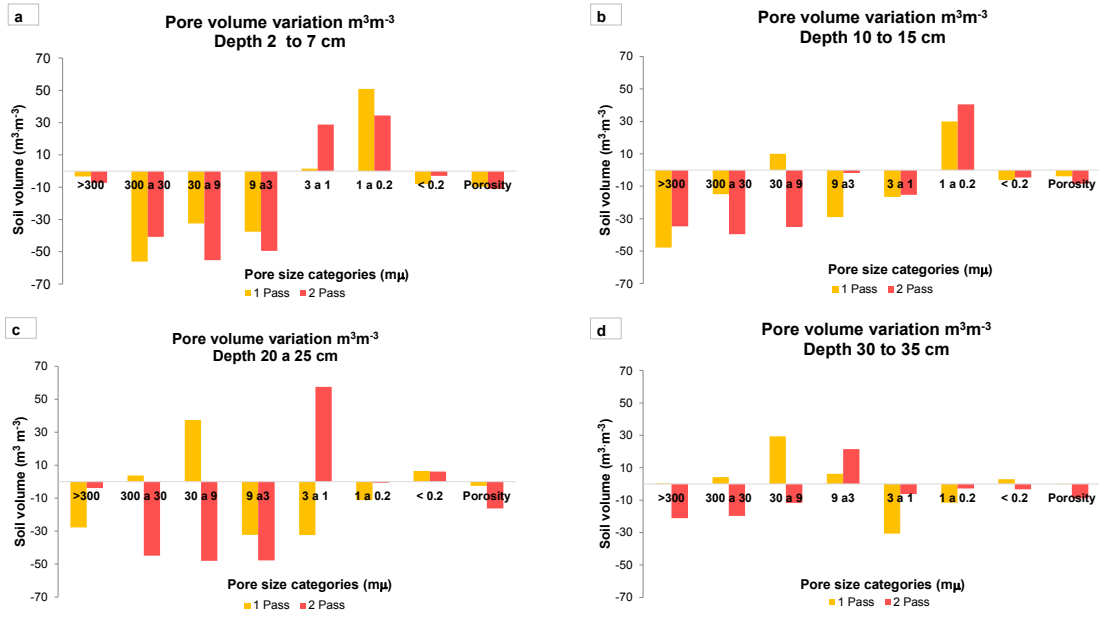

Fig. 4. Percentage variation in pore volume and saturated porosity relative to the control (no traffic) for each studied depth under one pass and two passes of the tractor-grain cart combination.

of pores into other size categories was observed, indicating pore loss rather than reorganization, which resulted in reduced porosity and was reflected in increased BD.

In the subsurface (20-35 cm), no changes in pore distribution were generally detected under 1P conditions. This layer, located below the plow layer, exhibited low soil moisture; under such conditions, stress tends to be transmitted horizontally, forming a supportive structural layer that prevents compaction in deeper horizons (Terminiello et al., 2004).

After 2P of the tractor-grain cart combination, a significant redistribution of pore structure and a loss of saturated porosity were observed. Under these conditions, the supporting effect of the plow layer was insufficient, and stresses transmitted to the subsurface exceeded its load-bearing capacity, leading to soil deformation (Schjønning et al., 2016). These results confirm the cumulative effect of machinery traffic (Seehusen et al., 2019; Augustin et al., 2020). Therefore, when using multi-axle equipment, traffic intensity should be considered a key parameter for predicting and preventing soil compaction.

In Fig. 5, SWRC illustrate that the effect of traffic decreases with depth. In the upper layer (0-15 cm), traffic treatments reduced water release within the tension range of 0 to -98 kPa (log h = 1.99), affecting pores larger than 30 μm. In contrast, in the 20-35 cm layers, these pore categories were only affected under the 2P treatment.

The flattening of the SWRC up to approximately -98 kPa (log h = 1.99 hPa) is attributed to the decrease in macroporosity, while changes in microporosity were minimal (Fig. 5). This behavior can be explained by the strong correlation of microporosity with soil texture and organic matter, whereas BD, which increases with traffic, shows a low correlation with microporosity (Rossetti and Centurion 2018).

Starting from -98 kPa, an increase in the slope of the SWRC was observed in the traffic-treated soils down to 15 cm depth, and in the 20-25 cm layer under the 2P treatment. This indicates greater water release at more negative matric potentials, resulting in increased resistance to water uptake by roots and reduced infiltration capacity due to the reduction in transmission pores. This change in slope suggests a redistribution of pore space, as observed in the analysis of percentage pore variation (Fig. 4), and in agreement with the findings reported by Moraes et al. (2018).

The parameter θ_i indicates the moisture content at the inflection point of the SWRC and is considered an indicator of optimal moisture for soil tillage (Dexter, 2004). The values of θ_i decreased with increasing traffic intensity, thereby reducing the window of opportunity for tillage operations. In the upper layer, a decrease in θ_i was already evident after 1P, whereas under 2P conditions this reduction extended throughout the entire profile studied (Table 5).

The S values obtained in the control were higher than the threshold proposed by Dexter (2004). However, Fernández et al. (2021) reported values greater than 0.09 for loamy soils, while da Luz et al. (2020) obtained values ranging from 0.05 to 0. 1 in clay soils and 0.06 to 0.13 in sandy soils. According to Dexter (2004), S values are influenced by soil texture, generally increasing as clay content decreases.

In Table 5, higher values of θ_i (i.e., lower matric suction at the inflection point) were associated with higher S-index values. Therefore, the reduction of the S-index is linked to a decrease in structural porosity, resulting in a vertical flattening of the SWRC (Dexter, 2004).

Fig. 6 displays S-index values plotted against DC, revealing a negative regression between the two variables across all soil layers. This trend can be explained by the reduction in macroporosity and the associated alteration of pore-size distribution. Similar findings were reported by Dexter (2004) in soils of different textural classes.

In this trial, S values below 0.035 were found only in the P2 treatment at 10-25 cm depth (Table 5). Although this supports the relationship between the S-index and soil structure, given that this layer coincides with the plow pan, values below 0.035 were also expected across all the studied layers in P2, as well as in the upper layers of P1.

A significant regression between S and DC was observed, with high R^2 values across most soil depths (Fig. 6). Only the depth 10-15 cm layer presented a moderate R^2. Overall, these results support the suitability of the S-index for characterizing soil structural quality in this system, in agreement with Fernández et al. (2021).

As observed in Fig. 6, S-index exhibited greater sensitivity to traffic, as a larger number of samples fell below the S threshold than exceeded the DC threshold. These results differ from those reported by Naderi-Boldaji and Keller (2016) and Al-Kayssi (2021), who mentioned greater accuracy for DC. However, to further validate the results of this study, additional soils should be evaluated and the relationships compared with crop yield data.

The traffic-induced pressure spikes were detected by the soil pressure sensors (Fig. 7). Two distinct peaks were observed at depths of 10 and 30 cm. In the upper layer, sensors recorded pressures of up to 45 kPa, with a 1.45-fold increase

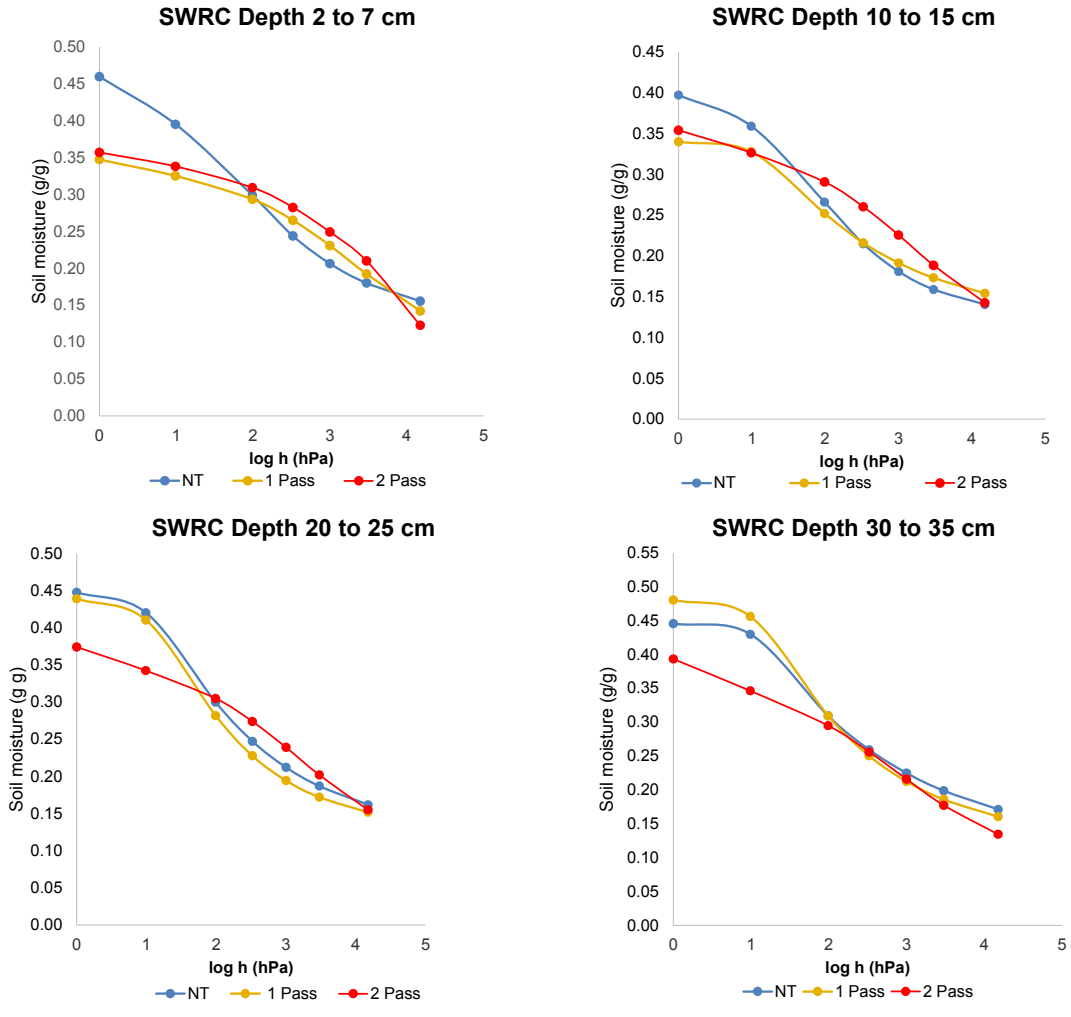

Fig. 5. Soil water retention curves relative to the control (no Traffic) for each studied depth under one pass and two passes of the tractor-grain cart combination.

in the traffic-treated plots. In both passes, residual pressure was recorded in the probes after the equipment had passed (Fig. 7).

These results were consistent with the observed increases in BD and DC values, which increased significantly under both traffic treatments. However, the second pass resulted in a lower pressure value, contrary to the expected increase (Table 6).

The formation of wheel tracks would be expected to increase pressure values during 2P due to the reduced distance between the tire and the sensor, along with the progressive soil structural deterioration during track formation (Shaffer et al., 2007). However, the shallow placement of the sensor probably made it susceptible to lateral displacement by the wheel load, allowing partial re-expansion of the surrounding soil volume. This effect could also have occurred during the second pass. Calleja Huerta et al. (2023) reported that pressure increments tend to decrease with successive passes until reaching stabilization point; under sufficiently high wheel loads, this stabilization may occur after two to three passes. In contrast, Shaffer et al. (2007) attributed this behavior to the progressive porosity reduction with each pass, allowing the soil around the sensors to bear more weight and facilitating a slight unloading of the sensors.

The pressure readings at 30 cm depth were similar (Table 6); however, residual pressure was observed only for 2P. These results are consistent with the DA and DC values, where no statistically significant differences were found in the 20-35 cm layer for 1P, whereas 2P showed significant increases in DA. The stresses generated by the

Table 5. S-index values and soil moisture content at the inflection point of the soil water retention curve (θ_i).

Depth	S			θ_i		
(cm)	NT	1 Pass	2 Pass	NT	1 Pass	2 Pass
2 to 7	0.047 b	0.036 a	0.037 a	0.30 b	0.20 a	0.21 a
10 to 15	0.047 b	0.038 ab	0.034 a	0.29 b	0.29 b	0.21 a
20 to 25	0.058 b	0.062 b	0.034 a	0.36 b	0.34 b	0.22 a
30 to 35	0.066 b	0.065 b	0.037 a	0.38 b	0.38 b	0.22 a

Different letters within the same row indicate significant differences among different tillage systems at the 0.05 probability level, according to Fisher's LSD test (5%) for S and the Kruskal-Wallis test (5%) for θ_i

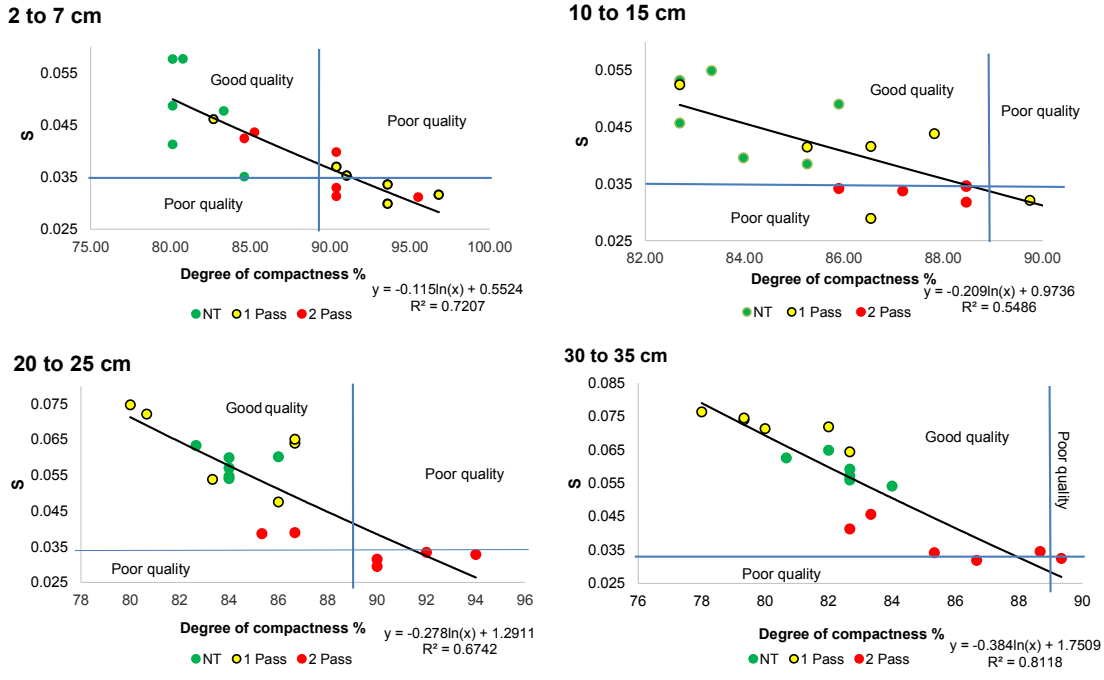

Fig. 6. Variation of the S-index in relation to degree of compactness for the four studied soil layers.

wheels exceeded the maximum capacity of the sensors (10.5 KPa); therefore, the total increases in the pressures of the probes could not be recorded. Keller et al. (2019) reported that wheel loads of 4 Mg can induce plastic deformation of the soil to depths of up to 30 cm. It should be noted that only the grain cart reached these load levels per wheel. Additionally, repeated traffic leads to cumulative loading effects (Seehusen et al., 2019; Augustin et al., 2020). Therefore, despite their measurement limitations, the sensors were effective in detecting plastic deformation and in capturing the intensity of the traffic.

CONCLUSIONS

A single pass of the equipment led to a significant increase in bulk density (BD) down to a depth of 15 cm. Under two passes, BD increased significantly from 20 cm to 35 cm depth.

Traffic affected drainage macropores, leading to the redistribution of pore volume toward storage pores associated with higher water-extraction tensions, accompanied by a loss of saturated porosity.

Subsurface porosity remained unaffected under 1P; however, under 2P, all pore categories larger than 9 μm were affected. In this treatment,

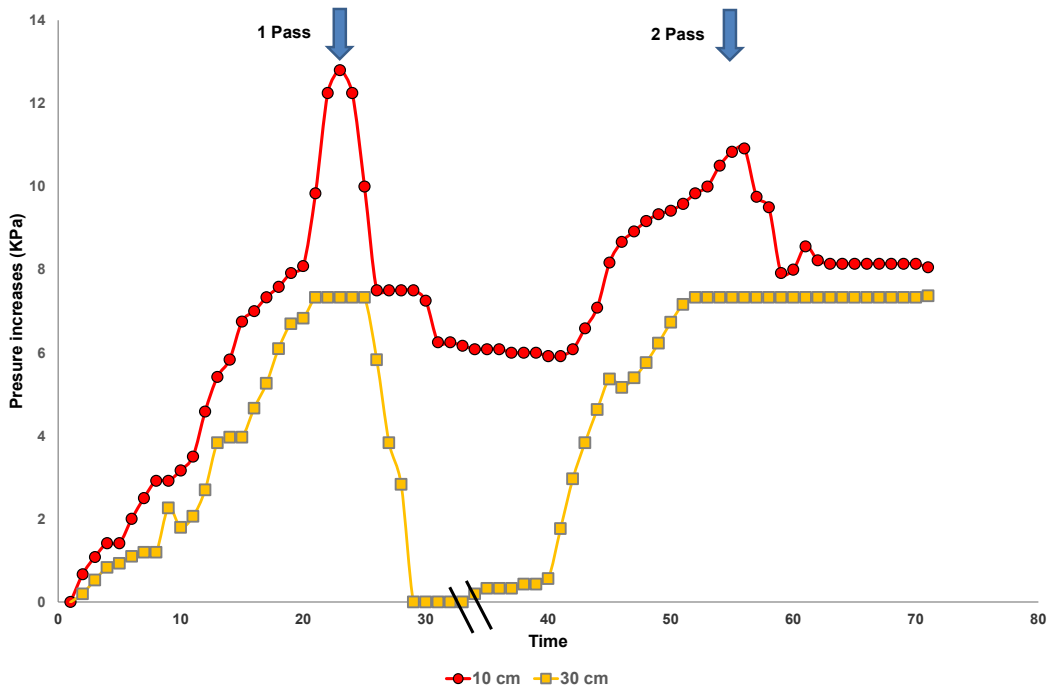

Fig. 7. Average normal soil stress measured with soil pressure probes at 10 and 30 cm depths during the first and second pass of the tractor- grain cart combination.

Table 6. Increase in soil pressure (KPa) measured by probes at different locations and depths under repeated traffic (first pass, 1P; second pass, 2P).

Depth	10 cm (HPS)		30 cm (LPS)	
Pass	1 P	2 P	1 P	2 P
Espartillar NT	12.58 b	9.17 a	7.35	7.68

Different letters in the same layer indicate significant differences between different tillage systems at the 0.05 probability level according to Fisher's LSD test (5%). HPS: high-pressure sensors. LPS: low-pressure sensors.

no pore-size redistribution was observed and a reduction in saturated porosity occurred.

The S-index reflected pore losses and redistribution similar to the porosity analysis, although the threshold value was only reached for the 2P treatment in the 10-25 cm layer. The DC values aligned with the change in trend of the curves obtained from the S vs. DC graphs, demonstrating the capacity of the S to assess soil degradation.

The pressure sensors detected vertical loads applied by the tires during wheel passage. Threshold values of CD and S-index were reached when residual pressure was recorded by the probes, demonstrating the potential of these indices to identify compaction levels that are detrimental to root growth. However, further research is required to validate these threshold values under different soil types and field conditions.

Author contributions

The following authors actively contributed to the literature review: Adrián Vallejos, Juan Galantini, and Pedro Bondía. Methodology development was carried out by Adrián Vallejos, Juan Galantini, and Pedro Bondía. Adrián Vallejos, Juan Galantini and Pedro Bondía contributed to the discussion of the results. Adrián Vallejos and Juan Galantini were responsible for reviewing and approving the final version of the manuscript.

ACKNOWLEDGEMENTS

We thank the Heffner family for providing their farm and agricultural equipment for the fieldwork (Saavedra district, Buenos Aires Province, Argentina).

LITERATURE CITED

Al-Kayssi, A. W. 2021. Use of water retention data and soil physical quality index S to quantify hard-setting and degree of soil compactness indices of gypsiferous soils. Soil and Tillage Research 206: 104805.

Aschonitis, V. G., E. Salemi, N. Colombani, and M. Mastrocicco. 2015. Comparison of different "S-index" expressions to evaluate the state of physical soil properties. Geological Engineering 33(4): 1055–1066.

Bellora, G., L. A. Lozano, C. Soracco, F. Guilino, N. Polich, M.P. Salazar, y Palancar. 2023. Tránsito repetido sobre la misma huella: efecto en las propiedades físicas de un argiudol típico. Ciencia del suelo 41(1): 1-16.

Botta, G. F., G. F Nardon, and R. Guirado Clavijo. 2022. Soil sustainability: Analysis of the soil compaction under heavy agricultural machinery traffic in extensive crops. Agronomy 12(2): 282. https://doi.org/10.3390/agronomy12020282

Botta, G. F., A.Tolón-Becerra, F. Bienvenido, D. Rivero, D. A. Laureda, A. Ezquerra-Canalejo. et al. 2018. Sunflower (*Helianthus annuus* L.) harvest: Tractor and grain chaser traffic effects on soil compaction and crop yields. Land Degradation & Development 29(12): 4252–4261.

Calleja-Huerta, A., M. Lamandé, O. Green, and L. J. Munkholm. 2023. Vertical and horizontal stresses from a lightweight autonomous field robot during repeated wheeling. Soil and Tillage Research 233: 105790.

Carter, M. R. 1990. Relative measures of soil bulk density to characterize compaction in tillage studies on fine sandy loams. Canadian Journal of Soil Science 70(3): 425–433.

da Luz, F., M. L. Carvalho, D. Aquino de Borba, B. E. Schiebelbein, R. Paiva de Lima, and M. R. Cherubin. 2020. Linking soil water changes to soil physical quality in sugarcane expansion areas in Brazil. Water 12(11): 3156. https://doi.org/10.3390/w12113156

Dexter, A. R. 2004. Soil physical quality: Part I. Theory, effects of soil texture, density, and organic matter, and effects on root growth. Geoderma 120(3–4): 201–214. https://doi.org/10.1016/j.geoderma.2003.09.004

Di Rienzo, J. A., F. Casanoves, M. G. Balzarini, L. Gonzalez, M. Tablada, and C. W. Robledo, 2019. InfoStat versión 2019. Centro de Transferencia InfoStat, FCA, Universidad Nacional de Córdoba Argentina. http://www.infostat.com.ar

Fernández, R., V. Belmonte, A. Quiroga, C. Lobartini, and E. Noellemeyer. 2021. Land-use change affects soil hydro-physical properties in Mollisols of semiarid Central Argentina. Geoderma Regional: 25 e00394. https://doi.org/10.1016/j.geodrs.2021.e00394

Fouladidorhani, M., M. Lamandé, G. Moitzi, M. M. Nawaz, and E. Arthur. 2025. Detection of negative consequences of traffic on subsoil properties depends on measurement type and scale: The case of a Calcaric Chernozem. Soil and Tillage Research 252: 106615.

Fu, Y., Z. Tian, A. Amoozegar, and J. Heitman. 2019. Measuring dynamic changes of soil porosity during compaction. Soil and Tillage Research 193 114-121

Guenette, K. G., G. Hernandez-Ramirez, P. Gamache, R. Andreiuk, and L. Fausak. 2019. Soil structure dynamics in annual croplands under controlled traffic management. Canadian Journal of Soil Science 99(2): 146–160.

Håkansson, I. 2005. Machinery-induced compaction of arable soils: Incidence, consequences, counter-measures. SLU, Department of Soil Sciences.

Iglesias, J. O., J. A. Galantini, H. Krüger, and S. Venanzi. 2014. Soil pore distribution as affected by cattle trampling under no-till and reduced-till systems. Agriscientia 31(2): 93-102.

Keller, T., M. Sandin, T. Colombi, R. Horn, and D. Or. 2019. Historical increase in agricultural machinery weights enhanced soil stress levels and adversely affected soil functioning. Soil and Tillage Research 194: 104293. https://doi.org/10.1016/j.still.2019.104293

Lima, C. L. R. D., P. B. Dupont, C. N. Pillon, and E. C. C. Miola, 2019. Least limiting water range, S-index and compressibility of an Udalf under different management systems. Scientia Agricola 77: e20170224. https://doi.org/10.1590/1678-992X-2017-0224

Moraes, M. T. D., R. Levien, C. R. Trein, J. D. A. Bonett, and H. Debiasi. 2018. Corn crop performance in an Ultisol compacted by tractor traffic. Pesquisa Agropecuária Brasileira 53: 464–477.

Naderi-Boldaji, M., and T. Keller. 2016. Degree of soil compactness is highly correlated with the soil physical quality index S. Soil and Tillage Research 159: 41–46. https://doi.org/10.1016/j.still.2016.01.010

Nawaz, M. M., M. A. Noor, H. Latifmanesh, X. Wang, W. Ma, and W. Zhang. 2023. Field traffic-induced soil compaction under moderate machine-field conditions affects soil properties and maize yield on sandy loam soil. Frontiers in Plant Science 14: 1002943. https://doi.org/10.3389/fpls.2023.1002943

Pozzolo, O. R., Ferrari, H. J., y Moltoni, A. F. 2006. Medidor dinámico de presiones ejercidas sobre el suelo por el tránsito de maquinarias agrícolas. En VII Congreso Latinoamericano y del Caribe de Ingeniería Agrícola (pp. 10–12). Chillán, Chile.

Raper, R. L., and F. J. Arriaga. 2007 Comparing peak and residual soil pressures measured by pressure bulbs and stress-state transducers. Transactions of the ASABE 50(2): 339–344. https://doi.org/10.13031/2013.22624

Rossetti, K. D. V., and J. F. Centurion. 2018. Use of S-index as a structural quality indicator for compacted Latosols cultivated with maize. Revista Caatinga 31(2): 455–465.

Schäffer, B., W. Attinger, and R. Schulin. 2007. Compaction of restored soil by heavy agricultural machinery–soil physical and mechanical aspects. Soil and Tillage Research 93(1): 28–43.

Schjønning, P., M. Lamandé, L. J. Munkholm, H. S. Lyngvig, and J. A. Nielsen. 2016. Soil precompression stress, penetration resistance and crop yields in relation to differently-trafficked, temperate-region sandy loam soils. Soil and Tillage Research 163: 298-308.

Seehusen, T., R. Riggert, H. Fleige, R. Horn, and H. Riley. 2019. Soil compaction and stress propagation after different wheeling intensities on a silt soil in South-East Norway. Acta Agriculturae Scandinavica Section B—Soil & Plant Science 69(4): 343–355.

Startsev, A. D., and D. H. McNabb. 2001. Skidder traffic effects on water retention, pore-size distribution, and van Genuchten parameters of boreal forest soils. Soil Science Society of America Journal 65(1): 224–231. https://doi.org/10.2136/sssaj2001.651224x

ten Damme, L., P. Schjønning, L. J. Munkholm, O. Green, S. K. Nielsen, and M. Lamandé. 2021. Soil structure response to field traffic: Effects of traction and repeated wheeling. Soil and Tillage Research 213: 105128. https://doi.org/10.1016/j.still.2021.105128

Terminiello, A. M., R. H. Balbuena, L. M. Draghi, J. A. Claverie, T. C. Palancar, e D. Jorajuría. 2004. Comportamento mecânico do solo sob tráfego em dois sistemas de preparo do solo. Engenharia Agrícola 24(1): 158–166.

Valente, I. Q. M., A. M. De Souza, G.S. Cassama, V. da Silva Bitter, J.A.S Parra, E.M Guimarães, and R.L.M Tavares. 2025. Changes in soil physical quality, root growth, and sugarcane crop yield during different successive mechanized harvest cycles. AgriEngineering 7(10): 325.

Van Genuchten, M. 1980. A closed-form equation for predicting the hydraulic conductivity of unsaturated soils. Soil Science Society of America Journal 44(5): 892–898. https://doi.org/10.2136/sssaj1980.03615995004400050002x

Wang, X., J. He, M. Bai, L. Liu, S. Gao, K. Chen, and H. Zhuang. 2022. The impact of traffic-induced compaction on soil bulk density, soil stress distribution and key growth indicators of maize in north China plain. Agriculture 12(8): 1220.

Yadav, G. S., R. Lal, and R. S. Meena. 2020. Vehicular traffic effects on hydraulic properties of a Crosby silt loam under a long-term no-till farming in Central Ohio, USA. Soil and Tillage Research 202: 104654. https://doi.org/10.1016/j.still.2020.104654